Chapter 11

Hierarchical Bayesian Modeling III: State-space models

Summary

This chapter is devoted to state-space models, *i.e.*, models with dynamic state transition in the latent layer of the hierarchical structure. Conversely to the examples presented in the previous chapters, unknown quantities of interest (*e.g.*, the number of fish, the biomass of a fish stock) evolve with time while observables only give a noisy piece of information about these latent variables. From a graphical modeling perspective, state-space modeling consists of adding arrows between variables within the hidden layer of a DAG so as to create the temporal link between these variables. To go one step further, state-space modeling consists of defining two key equations: the process equation with process noise that captures the stochastic dynamics of the hidden state variables, and the observation equation that relates the data at hand to the state variables, which may involve some observation noise. Surprisingly enough, statistical estimation under the Bayesian setting of (even complex) state-space models remains easily tractable. The flexibility of Bayesian analysis of state-space models is exemplified through two examples of growing complexities; both present educational qualities for illustrating the strengths and limits of the Bayesian analysis of state-space models. The first example sketches the dynamics of the biomass of a fish stock under fishing pressure. The model is used to derive estimates of key management parameters and to forecast changes in biomass under different management scenarios. The second example is an aged-structured population model for A. salmon. The model mimics the salmon life cycle with all its development stages, represented through a multidimensional state-space model.

11.1 Introduction

Modeling the system state dynamics is a critical issue encountered in many ecological applications such as population dynamics. Identifying the factors that control the system dynamics and being able to forecast its future evolution are key issues for the modeler.

In a state-space model, transition equations between state variables are used to sketch the dynamics of the system, and observation equations link the state variables to some observables. Such models with dynamic state transition in the latent layer of the hierarchical structure are encompassed in the general family of state-space models sometimes also referred to as hidden Markov models ([40]; [41]; [65]; [75]; [136]; [259]). From a graphical modeling perspective, the sophistication is a simple matter of adding arrows between variables within a hidden layer of a DAG to sketch the temporal link between the variables (see Figs. 1.12 and 1.14 in Chapter 1). Surprisingly enough, estimation under the Bayesian setting of (even complex) state-space models remains easily tractable.

To go further into details, state-space modeling consists of ascertaining two key equations (or set of equations): the process equation with parameters θ_1 and identically independently distributed *process noise* $\epsilon(t)$ that captures the stochastic dynamics of the hidden (not observed) state variables, Z_t, and the observation equation that relates the data at hand y_t to the state variables Z_t through an observation function involving parameters θ_2 and eventually some *iid observation noise* $\omega(t)$ (see also Chapter 1):

$$\begin{cases} Z_{t+1} = f(Z_t, \theta_1, \epsilon(t)) \\ y_t = g(Z_t, \theta_2, \omega(t)) \end{cases} \tag{11.1}$$

Using the convenient bracket notation of Chapter 1, Eq. (11.1) can also be written as:

$$\begin{cases} [Z_{t+1}|Z_t, \theta_1] \\ [y_t|Z_t, \theta_2] \end{cases} \tag{11.2}$$

where $[Z_{t+1}|Z_t, \theta_1]$ denotes the conditional pdf of state vector at time step $t+1$ given the state vector at time step t and parameters θ_1, and $[y_t|Z_t, \theta_2]$ denotes the conditional distribution of observation y_t given the state vector at time t and parameters θ_2.

As shown in Chapter 1 (Eq. (1.28)), once a prior $[Z_1]$ is specified for the state vector at the first time step, the joint prior distribution of θ_1 and $Z_{1:n} = (Z_1, ..., Z_n)$ can be written as in Eq. (11.3) below, thus

emphasizing the Markovian property in the state dynamics which defines the prior structure in the latent layer Z:

$$[Z_{1:n}, \theta_1] = [\theta_1] \times [Z_1] \times \prod_{t=1}^{n-1} [Z_{t+1}|Z_t, \theta_1] \tag{11.3}$$

Conditionally upon states Z_t and parameters θ_2, observations y_t are mutually independent and the observation equation also factorizes:

$$[y_{1:n}|Z_{1:n}, \theta_2] = \prod_{t=1}^{n} [Y_t = y_t|Z_t, \theta_2] \tag{11.4}$$

Following the general factorization of the joint posterior distribution for a Bayesian hierarchical model given in Eq. (1.25), the joint distribution of all state variables and parameters $\theta = (\theta_1, \theta_2)$ is straightforwardly obtained:

$$[Z_{1:n}, \theta|Y_{1:n} = y_{1:n}] \propto [\theta] \times [Z_1] \times \prod_{t=1}^{n-1} [Z_{t+1}|Z_t, \theta_1] \times \prod_{t=1}^{t=n} [Y_t = y_t|Z_t, \theta_2] \tag{11.5}$$

11.2 State-space modeling of a Biomass Production Model

11.2.1 Motivating example: The Namibian hake fishery

Let us consider as a first example the data from the Namibian hake fishery. Two hake species (*Merlucius capensis* and *Merlucius paradoxus*) are targeted by this fishery. The data analyzed here concern the fishery operating in zones 1.3 and 1.4 of the International Commission for the South-East Atlantic Fisheries (ICSEAF) from 1965 to 1988. For further details about the fishery shown in Fig. 11.1, we refer to the report from the International Commission for Southeast Atlantic Fisheries ([144]) or to [136] and [196].

The catch-effort data are presented in Table 11.1. The two targeted species are pooled in the dataset. The catches concern the total annual commercial catches of hakes (in thousand tons) realized by large ocean-going trawlers operating in the ICSEAF zones 1.3 and 1.4. The catches per unit effort data (CPUEs) are the catches per hours of fishing for a

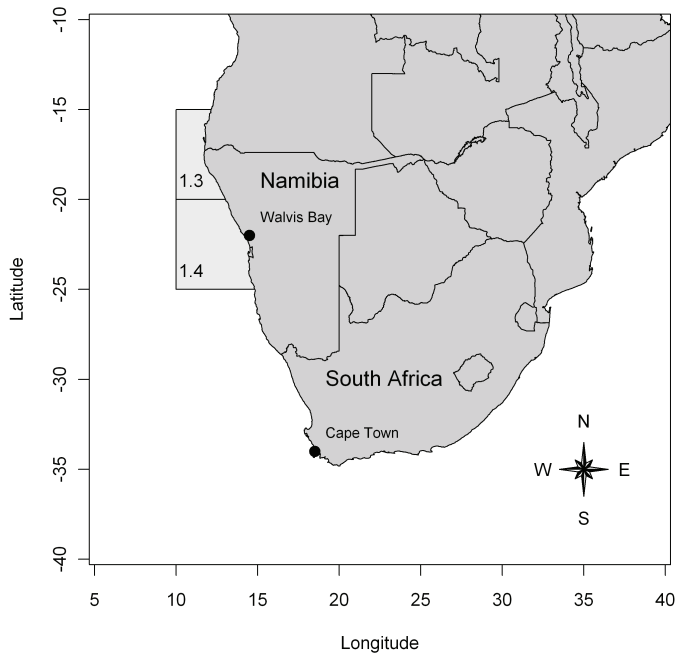

FIGURE 11.1: Location of the ICSEAF fishery areas 1.3 and 1.4 in the Southeast coast of Africa.

specific class of Spanish trawlers. As the CPUEs are standardized, they are considered here as a reliable index of abundance for the Namibian hake stock.

We rely on these data to model the dynamics of hake stock biomass through dynamic Biomass Production Models (BPM) (see also Figure 1.2, page 10). A dynamic BPM is a voluntarily crude but useful simplification of some harvested fish population dynamics ([137]; [244]) that only aims at helping fisheries scientists to interpret the data (*e.g.*, catches and abundance indices in Table 11.1). Analyzing data through BPMs allows to assess how the fishery pressure has impacted the biomass. For instance, it provides answers to questions such as:

- What is the maximum sustainable yield (C_{MSY}) and what are the past and current levels of yield sustainable with regards to the C_{MSY}?

Years	Catches	CPUE
1964	1.8	NA
1965	93.5	1.78
1966	212.4	1.31
1967	195.0	0.91
1968	382.7	0.96
...		
1984	228.7	0.64
1985	212.2	0.66
1986	231.2	0.65
1987	136.9	0.61
1988	212.0	0.63

TABLE 11.1: Catches and abundance indices for the Namibian Hake fishery in the ICSEAF Divisions 1.3 and 1.4 ([144]). Catches are in thousand tons. Catches per unit effort (CPUE) are in tons per standardized trawler hours. The data are reproduced after McAllister and Kirkwood [196].

- How large was the abundance in year 1988 (the last year for the dataset) with reference to its level when the fishery began?
- Could biomass level increase and yield be improved if more restrictive fishing quotas are imposed in the future?

The latter question is particularly important to test the performance of alternative management scenarios when efforts are being made to control the level of catches and promote sustainable harvest.

11.2.2 A state-space model for the biomass surplus production

The backbone of state-space modeling (SSM) of a BPM is to consider the time series of abundance indices as noisy observations of an underlying hidden process which mimics the dynamics of a fish stock biomass. Designing a SSM involves four steps:

1. Propose a mathematical model for the biomass dynamics including fishery removals;
2. Propose a model that sketches the noisy observation process;
3. Link these two components by a conditional structure;
4. Derive inferences using inverse (*i.e.*, Bayesian) reasoning.

11.2.2.1 Process equation for the underlying dynamics of the Biomass

The process equation models the underlying dynamics of the Biomass. The variable of interest is the total biomass in the population at each time t, denoted B_t. In BPMs with continuous time, the instantaneous change in the biomass level is modeled thanks to a differential equation which, when no exploitation occurs, can be written as:

$$\frac{dB_t}{dt} = h(B_t) \tag{11.6}$$

where $h(B_t)$ is the *production function*. It quantifies the balance between recruitment (arrival of new individuals in the stock biomass), growth (weight), natural mortality, and eventually emigration-immigration.

Maybe the most classical choice for the production function is the *logistic* equation, first proposed as a population model by P. F. Verhulst in 1938:

$$h(B_t) = r \times B_t \times (1 - \frac{B_t}{K}) \tag{11.7}$$

For simplifications of Eq. (11.7), the two parameters – the population intrinsic growth rate r and the carrying capacity K – are generally considered constant over time. The ecological theory behind such a model is that the production rate $\frac{1}{B_t} \times \frac{dB_t}{dt}$ will be maximum when the population stands at a very low level, and will decrease continuously (*e.g.*, because of intra-specific competition for the resource) when the size of the population increases. As no production occurs when $B = K$, K stands for the carrying capacity of the habitat. The dynamic BPM with the logistic production function is also known as the Schaefer biomass production model.

The dynamics can be modeled in discrete time, most often on a year-to-year basis. When fishing occurs, the biomass at the beginning of time step $t + 1$, denoted B_{t+1}, is obtained from B_t through a rather simple budget equation:

$$B_{t+1} = B_t + h(B_t) - c_t \tag{11.8}$$

where c_t is the observed harvest (in weight) between t and $t + 1$. When no catch occurs, it is easy to see that the biomass will stabilize at the virgin equilibrium level $B = K$.

A LogNormal random noise term is generally added to capture the biological variability due to (unpredictable) environmental variations. Hence, the stochastic version of the deterministic Eq. (11.8) is:

$$B_{t+1} = (B_t + h(B_t) - c_t) \times e^{\epsilon_{t+1}} \tag{11.9}$$

with ϵ_{t+1} a Normally distributed $N(0, {\sigma_p}^2)$ random term standing for the environmental noise (process error) with variance ${\sigma_p}^2$ in the log scale.

In a first approach, catches can be considered as observed without errors, and entered into the process equation (Eq. (11.9)) as observed covariates (hence the notation c_t with a lowercase letter). But catches could more realistically be considered as observed with some errors, or landings statistics can be systematically lower than true catches because many fish are discarded, landed illegally or the catches are simply misreported (see Hammond and Trenkel [128] for an example of a biomass surplus production model accounting for censored catches).

Equation 11.9 defines a stochastic Markovian transition which can alternatively be written as the probability distribution of the state variable B_{t+1} conditionally upon the previous state B_t, some parameters $\theta_1 = (r, K, \sigma_p)$ and the observed catches c_t. Following the notation used in Chapter 1, this Markovian transition will be written as:

$$[B_{t+1}|B_t, \theta_1; c_t] \tag{11.10}$$

nothing more than the general process Eq. (11.2) adapted to the biomass dynamics example.

To reduce the number of unknowns in the model and ensure statistical identifiability, one must set a constraint for the initial condition B_1. It is often assumed that the biomass at the beginning of the time series is a known proportion of the carrying capacity K. In the hake fishery, because catches were very low before the year 1964, it was assumed that the stock was not fished at the beginning of the time series. To be consistent with Eq. (11.9), the biomass of the first year was considered as LogNormally distributed around the carrying capacity K:

$$B_1 = K \times e^{\epsilon_1} \tag{11.11}$$

Let $t = 1, ..., n$ denote the time series for which observations are available (in what follows, we will often use *1:n* to denote the indices of the time series $t = 1, ..., n$). Conditionally upon the parameters $\theta_1 = (r, K, \sigma_p)$ (*e.g.*, those involved in the process) and upon the catches $c_{1:n}$, the sequence of unknown states $B_{1:n}$ follows a first-order Markov chain. The chain is initialized by Eq. (11.11). The transition kernel of the Markov process is defined by the dynamic process Eq. (11.10). Thanks to the conditional independence property, one can split the whole joint pdf into the product of single unit time steps. Once a prior distribution is specified for the parameters θ_1 and for the first state B_1 (conditionally upon θ_1, the prior $[B_1|\theta_1]$ is fully defined from Eq. (11.11)), the process equation can be factorized as Eq. (11.12) which is a specialized reformulation of the general process Eq. (11.3):

$$[B_{1:n}, \theta_1] = [\theta_1] \times [B_1|\theta_1] \times \prod_{t=1}^{t=n-1} [B_{t+1}|B_t, \theta_1; c_t] \tag{11.12}$$

11.2.2.2 Observation equation to link the data to the hidden process

The abundance indices $i_{t=1:n}$ are often assumed proportional to the current biomass $i_t = q \times B_t, \forall t \in \{1, ..., n\}$ with a catchability parameter q, considered constant over time. A common, although simplifying, supplementary assumption is that the relative abundance index of each year t is related to the unobserved biomass through a stochastic observation model:

$$i_t = q \times B_t \times e^{\omega_t} \tag{11.13}$$

with ω_t a Normally distributed $N(0, {\sigma_o}^2)$ random term representing the uncertainty in observed abundance indices due to measurement and sampling error (observation error). In addition, the ω_t are considered as mutually independent.

The observation Eq. (11.13) links the available data to the underlying dynamics. Following the notation used in Chapter 1, it defines the probability distribution of any abundance indice i_t conditionally upon the biomass B_t and the parameters $\theta_2 = (q, \sigma_o)$:

$$[i_t|B_t, \theta_2] \tag{11.14}$$

Equation 11.14 also defines the likelihood function, which gives the probability of the series of observations $i_{1:n}$ conditionally on the actual states $B_{1:n}$ and on the parameters θ_2. Conditionally on state B_t and parameters θ_2, the observations i_t are mutually independent, and the likelihood can be factorized as already shown in the general case in Eq. (11.4):

$$[i_{1:n}|B_{1:n}, \theta_2] = \prod_{t=1}^{t=n} [i_t|B_t, \theta_2] \tag{11.15}$$

It is not rare that fisheries scientists get more than one series of abundance indices to fit the model. For instance, as an additional source of information to the catch-per-unit-effort data in Table 11.1, other fishery-independent abundance indices might be available such as standardized CPUE from scientific surveys or abundance indices from acoustic scientific surveys. The information provided by additional abundance indices $i'_{1:n}$ can be easily integrated in the analysis by supplementing the observation Eq. (11.15) with conditional distributions $[i'_t|B_t, \theta'_2]$ associated with abundance indices $i'_{1:n}$ (see [195] or [197] for examples of SSM fitted to several abundance indices).

11.2.3 Deriving inferences and predictions

Combining the prior on the parameters $[\theta] = [\theta_1, \theta_2]$ with the process and the observation Eqs. (11.12) and (11.15) yields the full joint

distribution of the model. One recognizes the general factorization of a hierarchical model as explained in Eqs. (1.17) and (1.18):

$$\begin{aligned}[Parameters,&Process, Observables] \\ &= [Parameters] \\ &\times [Process|Parameters] \\ &\times [Observables|Process, Parameters]\end{aligned}$$

Applying Bayes' rule, the full joint posterior distribution of all unknowns is decomposed under the previous three terms as follows:

$$\begin{aligned}[B_{1:n}, \theta|i_{1:n}; c_{1:n}] & \\ &\propto [\theta] \\ &\times [B_1] \times \prod_{t=1}^{t=n-1} [B_{t+1}|B_t, \theta_1; c_t] \\ &\times \prod_{t=1}^{t=n} [i_t|B_t, \theta_2]\end{aligned} \tag{11.16}$$

The DAG of the model in Eq. (11.16) is given in Fig. 11.2. A sample of the full joint posterior distribution (Eq. (11.16)) can be easily obtained from MCMC sampling using WinBUGS software. The posterior distribution can be used to answer the following questions:

- What are the best guesses for the parameters (r, K) and the associated uncertainty?
- What are the credible values for the historical trajectory of the biomass $B_{1:n}$ and what is the level of the Biomass depletion over the time series $\frac{B_n}{B_1}$?
- What are the estimates for the management reference points C_{MSY} and B_{MSY} (directly derived from the parameters (r, K) following Eq. (1.5)) and their associated uncertainty?

Posterior predictive distributions can also be used to derive predictions of future trajectory of the biomass and catches over a time series $t = n+1, ..., n+k$ under alternative *management scenarios*. Simulations typically aim at comparing different harvest control rules, *e.g.*, different level of catches $c_{n+1:n+k}$.

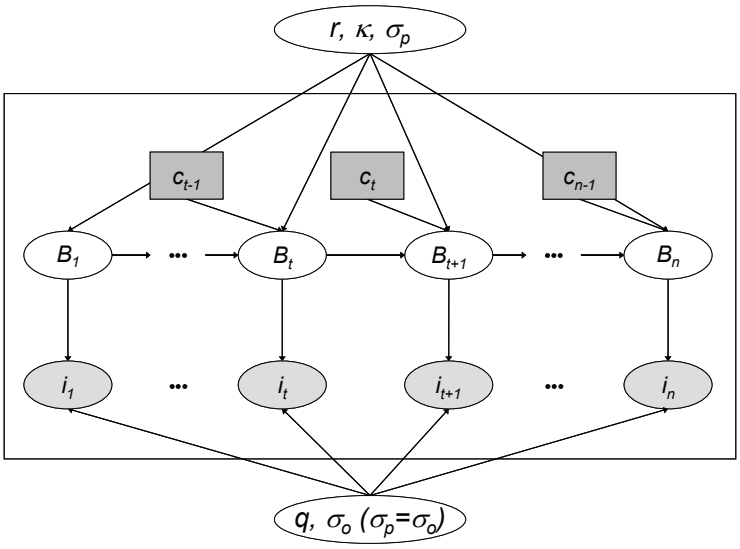

FIGURE 11.2: Directed acyclic graph of the state-space biomass production model.

11.2.4 Application to the dynamics of the Namibian hake stock

11.2.4.1 Additional hypotheses, priors and computational details

Back to the application to the Namibian Hake fishery, we now detail the additional hypotheses and some technical tricks that were made to fit the model.

To ensure that all parameters can be estimated, an additional hypothesis was formulated: the variance of the process and the observation errors were set to be equal. Indeed, the magnitude of process and observation errors σ_p and σ_o can hardly be specified a priori. But in the absence of any prior information on σ_p and σ_o, uncertainty in the data can be all transferred either in the process noise or to the observation noise, making it difficult to identify both variances precisely if they are totally set free a priori. Fixing the ratio of variances $\lambda = \frac{\sigma_p}{\sigma_o}$ is a classical additional trick used to reduce the number of unknown parameters. In the Bayesian setting λ would be equipped with a reasonably informative prior. However, it is worth noting that inferences in SSM are

seldom sensitive to the value of λ, unless it strongly favors observation or process error ([162]; [240]; [275]; [276]). Therefore, in the absence of any particular information on the relative magnitude of process versus observation error in the case of the Namibian hake fishery, $\lambda = 1$ was used as a default choice.

Fixing the process error variance σ_p^2 to 0 yields to the so-called *observation error model*, whereas fixing the observation error variance σ_o^2 to 0 yields to the so-called *process error model* ([240]; [275]).

As the data look informative, rather diffuse priors were set on the parameters $\theta = (r, K, q, \sigma^2)$ (Table 11.2).

Parameter	Prior
r	$\sim Uniform(0.01, 3)$
K	$\sim Uniform(100, 15000)$
$log(q)$	$\sim Uniform(-20, 20)$
$log(\sigma^2)$	$\sim Uniform(-20, 20)$

TABLE 11.2: Prior distributions on parameters of the biomass production state-space model applied to the Namibian hake fishery. The unit of the carrying capacity is in thousand tons. Following Millar [205], diffuse priors were assigned on q and σ^2.

Following Meyer and Millar [203], the dynamic state-space Eqs. (11.10) and (11.11) were reparameterized using the state variable $P_t = \frac{B_t}{K}$. Indeed, the parameter K and the latent state variables B_t are unknown but are in the same scale, *i.e.*, the scale of the absolute stock size. The constraint $B_1 = K \times \epsilon_1$ in Eq. (11.11) shows that conditionally upon a value of K, the scale of the whole time series of the biomass $B_{1:n}$ is fully determined. This dynamical structure induces a strong dependency between K and the whole biomass trajectory, which impedes an efficient exploration of the support of the posterior distribution by the Gibbs sampler. As shown by [202] and [203], using the new parameterization $P_t = \frac{B_t}{K}$ drastically improves the efficiency of the Gibbs sampler and the mixing speed of the MCMC chains.

For all estimations, three MCMC independent chains with dispersed initialization points were used. For each chain, the first 50,000 iterations were discarded. After this "burn-in" period, only one in 10 iteration steps (thinning) was kept to reduce the MCMC sampling autocorrelation. Inferences were then derived from a sample of 30,000 iterations obtained from three chains of 10,000 iterations. All the modeling results have undergone tests to assess convergence of MCMC chains. It is therefore assumed that the reported probability density functions are representative of the underlying stationary distributions, *i.e.*, the posterior pdf.

11.2.4.2 Inferences using the Schaefer-type production function

The posterior distributions of the key parameters are shown in Fig. 11.3 along with their main statistics in Table 11.3.

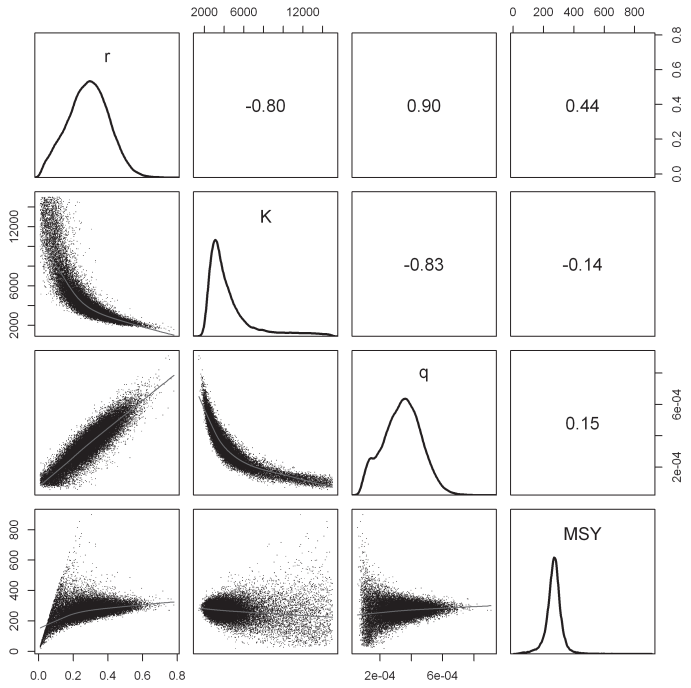

FIGURE 11.3: Posterior distributions of the key parameters obtained using the Schaefer-type production function. The marginal distributions are shown in the diagonal. Pairwise MCMC plots are shown in the lower part. The upper part shows the linear correlation between the MCMC draws.

The annual intrinsic growth rate is about 0.3 (Table 11.3), which is rather high and indicates that the stock should exhibit a high resilience to exploitation. The posterior median of C_{MSY} is about 268 (thousand tons), thus indicating that the stock was exploited above its optimal sustainable harvest rate during 10 years between 1968 and 1977.

Parameters (K, q) and (r, K) are highly negatively correlated, as shown by the joint MCMC samples in Fig. 11.3. The negative corre-

Parameter	Mean	Sd	2.5% pct.	Median	97.5% pct.
r	0.29	0.12	0.066	0.29	0.52
K	4500	2343	2225	3729	11790
q	0.00034	0.00012	0.00012	0.00034	0.00058
σ^2	0.0093	0.0032	0.0049	0.0087	0.017
C_{MSY}	266	53	152	268	364
B_{MSY}	2250	1172	1112	1864	5894
F_{MSY}	0.14	0.058	0.033	0.14	0.26

TABLE 11.3: Main statistics of the marginal posterior distributions of the key parameters obtained using the Schaefer-type production function.

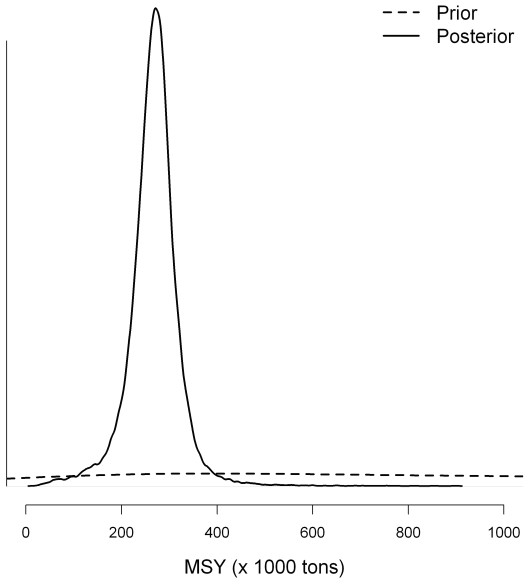

FIGURE 11.4: Prior and marginal posterior distribution of the Maximum Sustainable Yield (C_{MSY}) estimated using the Schaefer-type production function.

lation between K and q results from the structure of the observation Eq. (11.13). As the abundance indices $i_{1:n}$ are known, the data convey information about the product $q \times B_t$ (for the whole biomass trajectory $B_{1:n}$). As the biomass trajectory $B_{1:n}$ is scaled by parameter K, the parameters q and K can hardly be identified individually. Had an

informative prior been available for q or K, better inferences would have been obtained.

The negative correlation between r and K indicates that the data alone do not enable to clearly disentangle a very abundant population (large K) with a rather low growth rate r from one with a lower K but a higher r. However, the posterior distribution of the C_{MSY} (C_{MSY} is calculated from the product $r \times K$) is clearly updated by contrast with the prior (Fig. 11.4).

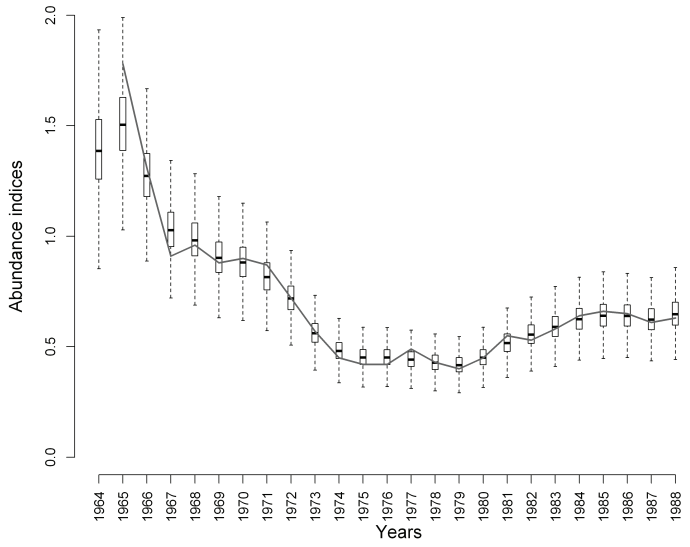

FIGURE 11.5: Quality of fit of the model with the Schaefer-type production function. The posterior predictive distributions of the abundance index (boxplot) are to be compared with the observed abundance index (solid line). No observed abundance index is available for year 1964.

To check whether the model reasonably fits the data, the posterior predictive of the abundance index for the whole time series (denoted $[\tilde{i}_{1:n}|data]$) were plotted together with the observed series of abundance index (Fig. 11.5). The joint posterior predictive of the abundance index was computed as:

$$[\tilde{i}_{1:n}|data] = \int_{\theta, B_{1:n}} [\tilde{i}_{1:n}|\theta, B_{1:n}] \times [\theta, B_{1:n}|data] \times d(\theta, B_{1:n}) \quad (11.17)$$

with

$$[\tilde{i}_{1:n}|\theta, B_{1:n}] = \prod_{t=1}^{t=n} [\tilde{i}_t|\theta, B_t] \tag{11.18}$$

and

$$log(\tilde{i}_t)|\theta, B_t \sim Normal(q \times B_t, \sigma^2) \tag{11.19}$$

As highlighted in Figure 11.5, the fit is pretty good. The fluctuations of the observed abundance indices over the time series are well captured by the predicted abundance indices. For the whole time series, the observed abundance indices are almost always contained in the predictive 50% Bayesian credibility intervals.

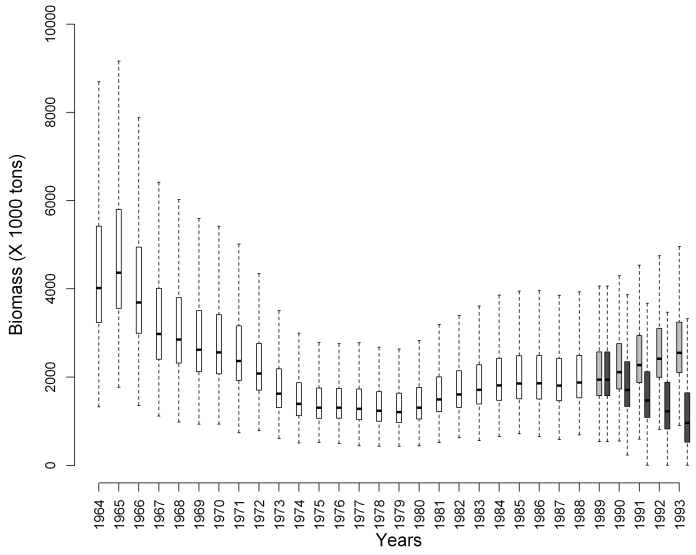

FIGURE 11.6: Marginal posterior distributions of the Biomass estimated using the Schaefer-type production function. Boxplots in gray fonts show the posterior predictive of the Biomass assuming a 100,000 tons constant quotas management option during 5 years after the year 1988, whereas boxplots in dark-gray are for quotas of 500,000 tons.

As a very interesting result, the model also provides estimates of the whole time series of the latent biomasses together with an appreciation of their uncertainty (Fig. 11.6). As previously shown, the shape of the time series of abundance indices is well reproduced. In 1964 (first year), the estimated biomass was about 4 million tons. From this time to the year 1972, the catches increased up to 606, 000 tons in 1972, and remained

higher than the estimated maximum sustainable yield up to 1977. Consequently, the Biomass decreases by a factor 2 and was estimated as less than 2 million tons in 1978. By this time, the catches were reduced by more restrictive management rules and the biomass started to rebuild.

As an additional result, two illustrative scenarios were run which enable to forecast the evolution of the biomass during 5 years (after 1988, the last year for which data are available) under two contrasted harvest rules (Fig. 11.6). The first one mimics constant catches of 100 thousand tons during 5 years, and the second one sketches constant catches of 500,000 tons. Forecasting indicate that harvesting 100,000 tons during 5 years will allow the biomass to increase again and lead to a very low risk of being at a biomass level less than B_{MSY} in 1993 ($[B_{1993} < B_{MSY}|Scenario\ 1] = 12\%$), whereas harvesting 500,000 tons (scenario 2) strongly affects the stock renewal and lead to a very high risk of serious depletion ($[B_{1993} < B_{MSY}|Scenario\ 2] = 94\%$).

11.2.4.3 Comparing the Schaefer-type versus Fox-type production function

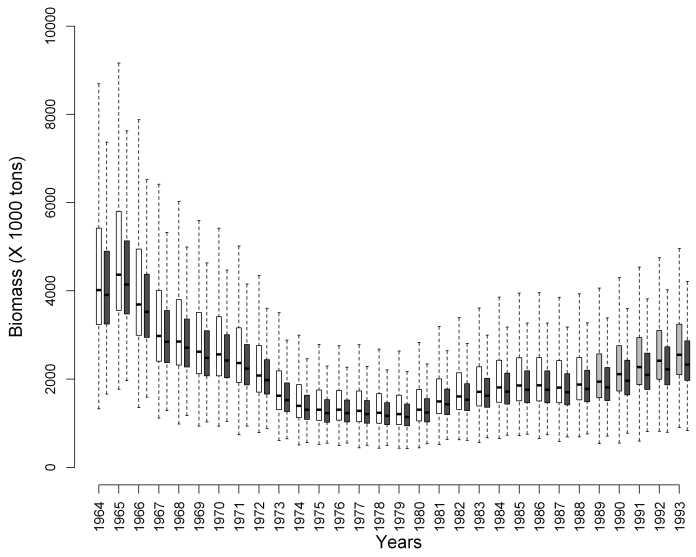

FIGURE 11.7: Marginal posterior distributions of the Biomass estimated using the Schaefer-type production function (gray font) and using the Fox-type production function (dark gray). The last 5 years are obtained assuming a $100,000$ tons constant quotas management option.

Consider now an alternative form for the production $h(B_t)$, the so-called Fox model ([137]; [244]):

$$h(B_t) = r \times B_t \times (1 - \frac{log(B_t)}{log(K)}) \tag{11.20}$$

and its associated fisheries management reference points:

$$\begin{cases} C_{MSY} = \dfrac{r \times K}{e^1 \times log(K)} \\ B_{MSY} = \dfrac{K}{e^1} \end{cases} \tag{11.21}$$

Figure 11.7 shows how the model behaves when the Fox-type production function is used instead of the Schaefer-type. The overall shape of the estimated biomass trajectory only differs slightly; the biomass estimated with the Fox production function being systematically lower than with the Schaefer one.

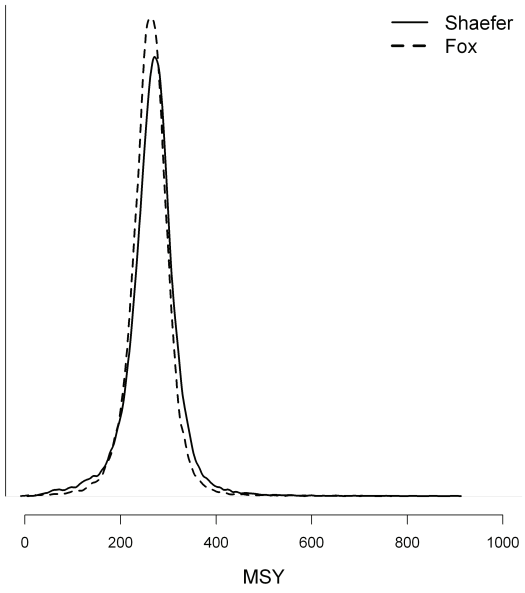

FIGURE 11.8: Marginal posterior distribution of the Maximum Sustainable Yield (C_{MSY}) estimated using the Schaefer-type (solid line) and the Fox-type (dotted line) production function.

As shown in Figure 11.8, both production functions lead to minor differences in the marginal posterior distributions of the maximum sustainable yield.

It is worth noting that both the Schaefer and the Fox production functions are particular cases of a more general equation with 3 parameters known as the *Pella-Tomlinson* production function ([244]):

$$h(B_t) = r \times B_t \times (1 - \frac{B_t}{K}^{m-1}) \tag{11.22}$$

Setting $m = 2$ yields to the Schaefer type production function (Eq. (11.7)), and $m = 1$ yields to the Fox production (Eq. (11.20)). However, only poor information generally exists in the dataset to estimate the parameter m, and the particular forms (Eqs. (11.7) or (11.20)) are generally preferred to Eq. (11.22).

11.3 State-space modeling of A. salmon life cycle model

In this section, we illustrate the flexibility of the Bayesian state-space modeling approach for stage-structured population dynamics models fitted to series of sequential observations of different nature. The example is inspired from Rivot *et al.* [259].

The method is applied to a fully stage-structured model for the Atlantic salmon life cycle with multiple life histories. The model describes the dynamics of the numbers of individuals at various life stages, with a discrete annual time step. It includes nonlinear regulation and has a probabilistic structure accommodating for both environmental and demographic stochasticity. The model is fitted to a dataset resulting from the comprehensive survey of the salmon population of the Oir River (Lower Normandy, France) between 1984 and 2001. Observation models are constructed to relate the field data to the hidden states at the various life stages. The observation process corresponds essentially to capture-mark-recapture (CMR) experiments for the evaluation of migrating juvenile and spawner runs and random sampling for demographic features. The ecological significance of the inferences is discussed at the end of the section.

Here, we largely rely on the A. salmon population ecology described in Chapter 1, but we take into consideration a more complete description of life histories: fish from the two smolt age classes (1+ Smolts and 2+